Into the first biomimetic sphingomyelin stationary phase: suitability in drugs' biopharmaceutic profiling and block relevance analysis of selectivity.

Giacomo Russo[1,2]*, Giuseppe Ermondi[3], Giulia Caron[3], Dieter Verzele[1], Frederic Lynen[1].

1. Separation Science Group, Department of Organic and Macromolecular Chemistry, Ghent University, Krijgslaan 281 S4-Bis, 9000 Ghent, Belgium.

2. School of Applied Sciences, Sighthill Campus, Edinburgh Napier University, 9 Sighthill Ct, EH11 4BN Edinburgh, United Kingdom.

3. CASSMedChem Research Group, Molecular Biotechnology and Health Sciences Department, University of Turin, Italy.

* corresponding author

To whom correspondence should be addressed:

Dr. Giacomo Russo

School of Applied Sciences

Sighthill Campus

Edinburgh Napier University

9 Sighthill Ct,

EH11 4BN Edinburgh, United Kingdom

Tel. +44 (0) 131 455 3464

e-mail: g.russo@napier.ac.uk

Into the first biomimetic sphingomyelin stationary phase: suitability in drugs' biopharmaceutic profiling and block relevance analysis of selectivity.

Giacomo Russo[1,2]*, Giuseppe Ermondi[3], Giulia Caron[3], Dieter Verzele[1], Frederic Lynen[1].

1. Separation Science Group, Department of Organic and Macromolecular Chemistry, Ghent University, Krijgslaan 281 S4-Bis, 9000 Ghent, Belgium.

2. School of Applied Sciences, Sighthill Campus, Edinburgh Napier University, 9 Sighthill Ct, EH11 4BN Edinburgh, United Kingdom.

3. CASSMedChem Research Group, Molecular Biotechnology and Health Sciences Department, University of Turin, Italy.

* corresponding author

Abstract

State of the art: Sphingomyelin (SPH) is a type of sphingolipid found in animal nerve tissues, especially in the membranous myelin sheath that surrounds some nerve cell axons. Because of its characteristics, SPH stationary phase represents an ideal tool to mimic the interactions taking place between active pharmaceutical ingredients and neurons.

Method: The IAM.SPH stationary phase (0.821 mg) was suspended in methanol (7.0 mL) and the resulting slurry packed (600 bar) in an HPLC column (10 cm x 2.1 mm). The column was operated at 300 μL min^{-1} at 25 °C using a mobile phase consisting of 60/25/15 (v/v/v) Dulbecco's phosphate buffer saline pH 7.4/methanol/acetonitrile. The elution was achieved isocratically and monitored by UV detection at 220 nm. The investigated dataset consisted of 88 compounds (36 neutrals, 26 bases and 26 acids). The block relevance (BR) analysis was accomplished starting by calculating 82 descriptors using the software VS+ and submitting the data matrices to Matlab. Multiple linear regression and related descriptors were obtained with Vega ZZ 64.

Results and discussion: The method developed allowed to achieve a solid and reproducible SPH affinity scale for the assayed compounds. Computational studies produced statistically significant models for the prediction and mechanism elucidation of the retentive behavior of pharmaceutically relevant compounds on the SPH stationary phase.

Conclusions: For ionizable compounds, the IAM.SPH exhibited an original selectivity when compared to the commercially available IAM.PC. Moreover, apart from its suitability to surrogate log BB, IAM.SPH was also found relate significantly with the drugs' fraction unbound in plasma, a crucial parameter in pharmacokinetics.

Keywords: sphingomyelin; immobilized artificial membrane; block relevance analysis; blood-brain barrier; biomimetic liquid chromatography; retention time prediction.

1. Introduction

Liquid chromatography has been successfully employed in both industry and academic research for fast, reliable, and reproducible of assessment of physico-chemical properties that are crucial in drug discovery and development programmes. For instance, Valkò and co-workers (Valko et al., 1997) used in a fast gradient reversed-phase HPLC method to derive a chromatographic hydrophobicity index (CHI) to be used as part of a protocol for high throughput physicochemical property profiling for rational drug design, whereas Natalini *et al.* (Natalini et al., 2009) have employed another chromatography derived index, *i.e.* φ_0, to model self-aggregation process of bile acids.

Immobilized artificial membrane (IAM) chromatography (Pidgeon et al., 1995; Pidgeon et al., 1991; Pidgeon and Venkataram, 1989) has been used since more than thirty years as a tool to scrutinize the interactions taking place between biological membranes and pharmaceutically relevant compounds. This comprises a type of reversed phase liquid chromatography implemented on stationary phases featuring phosphatidylcholine (PC) analogues which are covalently bound to silica (Ong et al., 1996). To date only three IAM stationary phases are commercially available: PC, PC.MG and PC.DD2 (Stewart and Chan, 1998), of which the latter (represented in Figure 1. A) is the most widely used (from here on out simply referred as IAM.PC). A conspicuous number of scientific reports (Grumetto et al., 2015, 2016a, b; Russo et al., 2017b, 2018) has successfully related IAM measurements to data of drugs' passage through complex biological barriers, including skin, intestinal mucosa and blood-brain barrier (BBB) achieved on *in vivo* or *in situ* models.

The BBB is a lipoidal membrane which protects the integrity of the central nervous system by segregating the brain and spinal cord parenchyma from the interstitial fluids (Pandey et al., 2016). It features a superior degree of leakiness as compared to barriers located elsewhere because of the presence of tight junctions, which impede any crossing from small polar compounds through the intercellular gaps (Van Bree et al., 1992). Although simplified, IAM models are constantly regarded as complimentary tools to avoid – or at least minimize – some animal testing when this is conducted for the assessment of drugs' pharmacokinetics, with an emphasis on membrane uptake (Ducarme, 1997). In this scenario, the IAM phases are designed and the experimental conditions optimized with the aim of mimicking the asset of the biological systems in which drugs' absorption takes place. Therefore, these platforms are claimed to be "biomimetic". However, the accuracy of IAM phases in mimicking the membrane barrier asset exhibited is severely constrained by some shortcomings (Ong et al., 1996). The most noticeable is that PC is only one of the phospholipids encompassing the BBB, whose composition features instead a wide range of lipids (Campbell et al., 2014). In fact, PC

represents only 28.7% (v/v) of the lipids composing the BBB, while other components are more abundant in this histologic structure. Among those, sphingolipids and cholesterol (together 54.2 % w/w) keep captivating the interest of the scientific community (Siakotos and Rouser, 1969). In fact, these lipids tend to segregate in discrete structures, called lipid rafts, whose role in cellular signalling, metabolism and trafficking is still very far from being completely unraveled (Bieberich, 2018; Kinoshita et al., 2018). Moreover, evidence suggests that these lipids accumulate specifically in the outer leaflet of the endothelial cells surrounding the brain parenchyma and hence are believed to be the structures that most readily interact with solutes passively diffusing from the circulating blood to the brain (Cannon et al., 2012). Although immobilization of these biological structures and their coupling to silica is challenging, their use in (high performance) liquid chromatography setups allows for superior robustness and reproducibility of the measurements.

Among the sphingolipids, sphingomyelin (SPH) is a type of sphingolipid found in animal cell membranes, especially in the membranous myelin sheath that surrounds some nerve cell axons (Slotte, 2016). It usually consists of phosphocholine and ceramide, or a phosphoethanolamine head group. In humans, SPH represents ~85% of all sphingolipids, and typically make up 10–20 mol % of plasma membrane lipids (Garcia-Arribas et al., 2016). However, SPH % in the BBB equals 33.4%, being the most abundant lipid in this strategic body district (Siakotos and Rouser, 1969).

SPH stationary phases designed for IAM chromatography are not commercially available. However, in 2011, a prototype SPH stationary phase for IAM chromatography was synthesized by an ultra-short, solid-phase inspired methodology (Verzele et al., 2012), in which an oxidative release monitoring strategy played an essential role. This prototype was evaluated in a proof-of-concept model for BBB passage (De Vrieze et al., 2014). However, while there is a conspicuous amount of literature aimed at modeling (Taillardat-Bertschinger et al., 2002), and at some extent predicting (Russo et al., 2017a), the retention of chemically diverse solutes on the IAM.PC phases commercially available, no data is available so far with regards to prediction and mechanism elucidation of analytical retention on IAM phases based on SPH. This article is meant as a contribution to fulfilling this demand using the block relevance (BR) analysis (Ermondi and Caron, 2012; Ermondi et al., 2014) and quantitative-structure-property relationships (QSPR) (Pedretti et al., 2004) , a chemometric tool designed for the stationary phases selectivity characterization.

We have four main aims: (*i*) collecting a good number of experimental data to build up a SPH affinity database of pharmaceutically relevant compounds; (*ii*) providing mechanistic information concerning the nature of the intermolecular forces driving retention on this novel prototype; (*ii*) assessing analytical retention similarities and dissimilarities with regards to the IAM phases commercially available to evaluate if further implementation of such phases is advantageous (*iii*) allowing prediction of chromatographic retention factors on the IAM.SPH and (*iv*) investigate the relevance of this novel stationary phase in drug development

programs dealing with the screening of new chemical entities according to their potential to cross biological membranes.

To reach our aims we firstly determined experimental data by LC conducted on the IAM.SPH phase, then applied BR analysis to obtain the mechanistic interpretation of IAM.SPH data. Briefly, the BR strategy is based on a PLS algorithm and VolSurf+ (VS+) descriptors (Ermondi and Caron, 2012). It pools the 82 VS+ descriptors into six easy-to-interpret blocks and graphically shows the relevance of a certain block in the PLS model: the higher the value, the more significant the block. The organization of the VS+ descriptors in blocks allows a straightforward understanding of the investigated phenomena (*e.g.* chromatographic retention, partitioning) because the six blocks provide an easy mechanistic interpretation based on the nature of the interaction of the solute with the environment represented by some tailored probes defined by the GRID methodology. BR analysis also allowed to compare the retention of the IAM.SPH phase with that observed on the commercially available IAM.PC columns to highlight similarities and dissimilarities.

A second computational strategy strategy based on 27 descriptors and multiple linear regression (MLR) algorithm, was also set-up to build models allowing to produce some sort of chromatographic behavior prediction. This is very relevant in drug discovery programs. In fact, although extremely high degrees of accuracy are hardly achievable, statistic models can complement other druggability assessment technologies and act as a filter in screening extremely large and complex compound libraries for their ability to cross the BBB and be up taken by the brain. Indeed, combinatorial synthetic approaches (Marakovic and Sinko, 2017) are nowadays able to generate a huge number of compounds at an incredibly fast rate and the screening demands for such ample libraries are currently unmet in most cases. In these scenarios, pharmaceutical enterprises might decide to compromise between accuracy and speed, with the aim of channelling their drug design efforts in a direction that is safer to a solid extent.

Finally, the relevance and suitability of the IAM.SPH phase in ADME profiling, with an emphasis on absorption, distribution, and BBB permeability, was also scrutinized by retrieving literature pharmacokinetic data.

2. Materials and methods

2.1 *In vitro* measurements

2.1.1 Chromatographic columns

The experiments were performed on a IAM.SPH (10 µm, 100 mm × 2.1 mm 300 Å pore size) analytical column prepared in house as described in 2.1.3. A subgroup consisting of 36 neutral compounds were also tested on a IAM.PC.DD2 column (10 µm, 100 x 4.6 mm 300 Å pore size, Regis Technologies, Inc Morton Grove, IL, USA).

2.1.2 Chemicals

The solutes were obtained from Merck Millipore (Machelen, Belgium, previously known as Sigma-Aldrich), TCI-Europe (Zwijndrecht, Belgium), Thermofisher Acros Organics (Geel, Belgium), Cerilliant Corporation (Round Rock, TX) and Aurora Fine Chemicals Ltd - Europe (Graz, Austria) as listed in Table 1 and S1. Their purity was equal to or higher than 98%.

2.1.3 Column packing

The IAM.SPH stationary phase (0.821 mg), previously synthesized (Verzele et al., 2012), was suspended in methanol (7.0 mL) and the resulting slurry packed (600 bar) by a Haskel airdriven pump (Burbank, CA) in an HPLC column (100 x 2.1 mm).

2.1.4 Column performance assessment

Twelve model drugs, *i.e.* acetaminophen, amitriptyline, atenolol, benzene, carbamazepine, chlorpromazine, cimetidine, desipramine, ethylbenzene, ibuprofen, propranolol and ropinirole, covering a retention time range spanning from 1.2 to 90.2 minutes were determined on the SPH stationary phase prototype and compared with the data already published (Verzele et al., 2012) to verify column reproducibility. Experimental conditions are the same as reported in (Verzele et al., 2012), except for the UV wavelength which was set to 220 nm for all the dataset. Results are reported in the supporting information section. A plot of experimental vs published is displayed in Figure S1, while the retention data are listed in Table S1. The high degree of accuracy (r^2 = 0.96) is clear indication that the performance of the stationary phase was preserved and therefore the column was used for the study. However, the analytes acetaminophen, atenolol, cimetidine and ropinirole exhibited some minor fluctuations when compared to already published data.

2.1.5 HPLC measurements (IAM.SPH)

IAM.SPH chromatographic analysis was performed on an Agilent 1100 (Santa Clara, CA, USA). The system included a quaternary pump, a micro vacuum degasser, a column thermostat and an automatic injector. An

Agilent 1100 Series variable wavelength detector was used and set at 220 nm. The separation was carried out at 25 °C, the flow rate was 300 μL min^{-1} and the injection volume was 10 μL. The autosampler needles were washed with 50/50 (v/v) 2-propanol/water solution every three runs to avoid any cross contamination and a blank run was done every five injections. All the analyses were performed at least in triplicate and the results reported are the average of at least three analytical determinations.

2.1.6 Mobile phase and sample preparation

Water (18.2 MΩ·cm^{-1}) was purified and deionized in house via a Milli-Q plus instrument from Millipore (Bedford, New Hampshire, USA). IAM.SPH mobile phases consisted of a solution 60/25/15 (v/v/v) Dulbecco Phosphate Buffered Saline (DPBS) / methanol /acetonitrile (both HPLC grade Biosolve, Valkenswaard, The Netherlands). DPBS was composed of 2.7 mmol·L^{-1} KCl, 1.5 mmol·L^{-1} potassium dihydrogen phosphate, 137.0 mmol·L^{-1} NaCl, and 8.1 mmol·L^{-1} disodium hydrogen phosphate (Merck). The pH was adjusted with sodium hydroxyde and the aqueous solution had a pH value of 7.40 ± 0.05. The IAM.PC mobile phase was composed of a 10 mM ammonium acetate buffer (Merck Millipore, Machelen, Belgium, previously known as Sigma-Aldrich, purity $\geq$ 98 %) and acetonitrile (Merck Millipore, HPLC grade) in ratios spanning between 0 and 30% (v/v) and extrapolated to 100% aqueous eluents by an extrapolation method (Braumann et al., 1983).

The mobile phase was *vacuum* filtered through 0.20 μm nylon membranes (Grace, Lokeren, Belgium) before use. Stock solutions of all drugs were prepared by dissolving 10 mg in 2 mL of methanol except for quinidine and quinoline for which stock concentrations of 1 mg mL^{-1} was used. Caffeine and pentoxifylline were dissolved in water (5 mg mL^{-1}), the stock solution of domperidone was prepared in dimethyl sulfoxide (5 mg mL^{-1}) , chlorpromazine, diethylstilbestrol, estradiol and tolnaftate were dissolved in acetonitrile (5 mg mL^{-1}), hydrocortisone and hydrocortisone 21- acetate were dissolved in ethanol (2.5 mg mL^{-1}). Stock solutions were stored at 4 °C, except for atenolol, chlorambucil, nifedipine, rifampicin and testosterone which were stored at −20 °C. Working solutions were freshly prepared at the beginning of each day by dilution of the stock solutions to 50 μg mL^{-1} with mobile phase for all the analytes, except for tolnaftate and diethylstilbestrol which were diluted to 25 μg mL^{-1} with a 50/50 (v/v) water/acetonitrile solution. Nifedipine, nitrofurantoin and rifampicin working solutions were wrapped in aluminium foil before feeding the autosampler to protect these chemicals from photodegradation.

2.1.6 HPLC measurements (IAM.PC)

IAM.PC measurements of the 36 neutral compounds were accomplished as described in a previous paper (Ermondi et al., 2018).

2.2 *In silico* calculations

2.2.1 Processing

The chromatographic retention coefficients of each analytes were calculated by using the following expression:

$$k = \frac{t_r - t_0}{t_0} \quad \text{Eq. (1)}$$

in which t_r is the retention time of the compound of interest and t_0 the retention time of a non-retained compound (acetone). All reported log k values are the average of at least three measurements; for each log k value the 95% confidence interval associated with each value never exceeded 0.04.

2.2.2 Datasets

Compounds were organized in 4 datasets: a) the complete dataset including all the 88 compounds (called Dataset), b) a dataset of 36 neutrals compounds firstly assayed by Lombardo *et al.* (Lombardo et al., 2000) (named Neutrals), c) a dataset of 26 acidic compounds (named Acids), d) a dataset of 26 bases (named Bases).

2.2.3 BR analysis

BR analysis was accomplished as detailed elsewhere (Ermondi and Caron, 2012; Ermondi et al., 2014; Vallaro et al., 2020). The SMILES codes of the 88 compounds were used as an input for VS+ software. The electrical state was assigned by pK_a calculations implemented in the software and an average conformation was build and minimised.The 82 descriptors directly obtained from 3D molecular interaction fields (MIFs) were then calculated (Ermondi and Caron, 2019; Goetz et al., 2017). The four data matrixes (one for each datasets) including descriptors and chromatographic data were submitted to Matlab (ver. R2019a, https://it.mathworks.com/) to perform Partial Least Square Regression (PLSR) and VIP analysis. As already discussed elsewhere (Ermondi and Caron, 2012), since here the PLS model is used for interpretative and not predictive purposes, only internal validation was performed.

Finally, an in-house Matlab script grouped the descriptors in blocks and processed the corresponding VIPs to draw the BR plots

Processing was done on a notebook equipped with a 4 cores Intel i7-4700MQ and 12 GB of RAM operating with Windows 10.

BR analysis interpretation is obtained by two graphical outputs: a) the *absolute BR plot* that shows the relevance of any block to the PLS model independently of the sign (the higher, the more relevant) and b) the *BR plot with signs* which splits the contribution of any block into positive BR (+) and negative BR (-) portions. BR (+) indicates how much the considered block favours the considered descriptor (e.g. log k $^{IAM.SPH}$) whereas BR (-) shows how much the block lowers the descriptor. Blocks with small and comparable positive and negative contributions indicate the high noise and inter-correlation of the descriptors of the block itself and thus are poorly relevant in the description of the investigated phenomenon.

2.2.4 QSPR modeling

MLR analysis was accomplished by VEGA ZZ x64 software 3.2.0.9 (Pedretti et al., 2004) implemented on a one 8 core i7 at 3.1 Ghz CPU and 32 GB of RAM Windows machine. Physico-chemical and topological properties (Virtual log P (Gaillard et al., 1994), lipole (Pedretti et al., 2002), volume, polar surface area, surface accessible to the solvent, gyration radius, ovality, mass, number of atoms, angles, dihedrals, etc) were calculated by VEGA ZZ software and finally, all molecules were inserted into a Microsoft Access database. Detailed information is reported in here (Russo et al., 2017b). In brief, The starting three-dimensional structures of the considered molecules were downloaded from PubChem database (Kim et al., 2019; Kim et al., 2016), and they were considered in both zero atomic charge and ionized form. The Gasteiger−Marsili method (Gasteiger and Marsili, 1980), along with CHARMM force field (Brooks et al., 2009; Brooks et al., 1983; MacKerell et al., 2002), was applied to calculate the atomic charges. After that, structures were minimized by AMMP software (Harrison, 1993) (conjugate gradients, 3000 iterations, toler 0.01). The best independent variables were selected by calculating the correspondent equation with a single regressor. Regressions with r^2 value less than 0.10 determine automatically the exclusion of the independent variable. Collinear independent variables were identified by calculating the Variance Inflation Factor (VIF) value for each regressor pair. Variable pairs with VIF > 5.0 were not considered in the model calculation. Calculation of the models with a number of regressors from one to four. Statistic models were developed by using either the zero-charge or the ionized forms of the compounds. To take into account the distribution of the microspecies at the experimental pH, a weighted average of the physico-chemical descriptors at the experimental pH according to the experimental pK_a values was also performed. For each model, a cross-validation procedure (leave-one-out) is performend and the prediction power is shown as q^2. Validation was performed on the dataset by the model validator script that splits randomly the whole dataset in a number of training and test set pairs. For each training set, the regression coefficients are calculated to evaluate the

test set in terms of standard deviation of errors, angular coefficient, intercept and r^2 of the trend line of the chart of the predicted *vs.* experimental activities. A number of 18 and 8 were selected as size of the test set and number of trials, respectively.

2.2.5 Postprocessing

Plotting and data analysis was done by Microsoft Excel for Office 365 v 16.0 at 64 bit.

2.3 Literature data sources

For the dataset "neutrals" , experimental lipophilicity values (log $P^{n\text{-oct/water}}$) were taken from Lombardo and co-workers (Lombardo et al., 2000). For the ionizable molecules (*i.e.* datasets Acids and Bases), they were taken from DrugBank (Wishart et al., 2018), except for verapamil, 4-amino benzoic acid, celecoxib, chlorambucil and fexofenadine, whose source was PubChem (Kim et al., 2016). Chromatographic retention data achieved on both IAM.PC and IAM.SPH stationary phases in the same experimental conditions were gathered from (De Vrieze et al., 2014). *In vivo* data of membrane passage were collected from (Avdeef, 2012), while *in vitro* PAMPA BBB measurements were used from (Tsinman et al., 2011). The reference report *in vivo* data assayed on various species including rat, mouse, pig and human. Although values on different species were claimed by the authors to be highly interrelated, we averaged them for the sake of consistency.

3. Results and discussions

3.1 IAM.SPH determinations

3.1.1 IAM.SPH performance assessment

Before starting the study, twelve model drugs were tested on the IAM.SPH analytical column to assess data reproducibility and the measurements were compared to those reported in (De Vrieze et al., 2014). A dataset featuring wide SPH affinity (log $k^{IAM.SPH}$ from -0.539 to 2.110) and spanning different lipophilicity degree (log $P^{n\text{-octanol/water}}$ from 0.16 (atenolol) to 5.90 (chlorpromazine)) and ionization (neutrals, acids and bases included) was selected. The results were evaluated in terms of reproducibility as compared to the published data (De Vrieze et al., 2014), intraday and interday precision. Regarding the former, a very high squared correlation coefficient (r^2 = 0.96) was achieved and no elution order changes were observed. This implies that

315 performance of the IAM.SPH stationary phases was preserved and that no anormalities during packing and
316 re-equilibration took place. As to the second, the % standard deviation (intraday precision) was retention
317 time independent and below 3% for all the measurements as reported in Table S1. The interday precision
318 was instead below 5% (data not shown).

319

320 **3.1.2 IAM.SPH and IAM.PC systems: relationships with *n*-octanol/water lipophilicity**

321 The LC determinations were conducted isocratically and some exemplative chromatograms are reported in
322 Figure 2. Although the use of a gradient could speed up the process, we needed to collect data to build QSPR
323 models which required thermodynamic experimental descriptors. The identification of the mobile phase was
324 not trivial since the use of 30% (v/v) methanol as organic modifier as in our previous study (De Vrieze et al.,
325 2014) did not allow any elution of some highly lipophilic compounds, *i.e.* tolnaftate and diethylstilboestrol.
326 Therefore, a more apolar organic modifier ratio equal to 25/15 (v/v) methanol/acetonitrile had to be used.
327 The addition of acetonitrile was beneficial as it allowed a solid lowering in the operating pressure by reducing
328 the viscosity of the mobile phase. Nevertheless, the two most lipophilic compounds (tolnaftate and
329 diethylstilboestrol) eluted after 94.0 and 52.0 minutes, respectively.

330 Interestingly, highly lipophilic neutral solutes, such as diethylstilbestrol and tolnaftate, have superior affinity
331 on the IAM.SPH (log $k^{IAM.SPH}$ values are 1.672 and 1.928, and log $P^{n\text{-oct/water}}$ equal to 5.10 and 5.09, respectively)
332 as compared to bases of similar lipophilicity, for instance chlopromazine (log $k^{IAM.SPH}$ is 0.891 and log $P^{n\text{-oct/water}}$
333 equals 5.90). This occurrence highlights some interesting differences between IAM.PC and IAM.SPH. Indeed,
334 based on some partitioning experiments undertaken on liposomes, Alex Avdeef formulated the so-called “pH
335 piston hypothesis” (Avdeef et al., 1998) that was soon after extended to IAM.PC phases. According to his
336 theory, cations would be favored with regards to neutral compounds of same lipophilicity in the interaction
337 with IAM.PC phases as its negatively charged phosphate moieties locate more internally as compared to the
338 positively charged amino groups. This allows bases to have a deeper and more productive interaction of
339 electrostatic nature and to better accommodate their apolar moieties in the hydrophobic tails of the lipid
340 network, especially as compared to acidic solutes. Anions, on the contrary, can engage dipolar interplay with
341 the positively charged amino groups lying in the distal part of the stationary phases, much further from the
342 silica core. This results in a more superficial and weaker interaction that effects in acids being retained less
343 than neutral isolipophilic molecules. Diethylstilbestrol and tolnaftate when compared with chlorpromazine
344 support that retention on the IAM.SPH does not seem to comply with the “pH piston hypothesis” and this
345 depicts a rather different selectivity as compared to the IAM.PC on the market. Figure 3 generalizes the lack
346 of fulfilment to the “pH piston hypothesis” exhibited by the IAM.SPH system. In fact, the plot shows that the
347 presence of ionizable moieties mostly acts as a disturbing agent, at least in a “pharmaceutically relevant” log

348 $P^{n\text{-octanol/water}}$ range (-1.0 - +5.0). Indeed, on IAM.PC phases extensively ionized acids are retained significantly
349 less, while bases interact more readily instead as compared to neutral molecules exhibiting similar
350 lipophilicity.

351 Overall, although some exceptions can be observed, the collected data suggest:

352 1. Analogously to partitioning on IAM.PC phases (Grumetto et al., 2014), log $k^{IAM.SPH}$ values of neutral
353 compounds relate unambiguously with log $P^{n\text{-octanol/water}}$ by a highly significant linear relationship (r^2 =
354 0.95 and Figure 3a);
355 2. This dependency is disrupted when solutes ionize and specifically the interaction rank on the
356 IAM.SPH is neutral>acids>bases;
357 3. The affinity for the IAM.SPH of ionizable chemicals depicts interactions which differ from the
358 "classical" *n*-octanol/water lipophilicity.

359 The last statement is motivated by the aspect that rough relationships between log $k^{IAM.SPH}$ and log $P^{n\text{-}}$
360 $^{octanol/water}$ are seen for both acidic (r^2 = 0.64) and basic (r^2 = 0.62, in both cases data not shown) compounds.

361

362 However, our measurements were conducted at a relatively high ratio of organic modifier, *i.e.* 40% (v/v), that
363 could affect retention in multiple ways. For instance, by lowering the dielectric constant of the eluents, the
364 difference in polarity between stationary and mobile phase decreases, hence resulting in a lower retention.
365 Moreover, the addition of organic modifier also decreases the acidic/basic strength of the ionizable solutes
366 to an extent that is dependent both on the chemistry of the compound and on the characteristics of the
367 solvents employed (Rossini et al., 2018).

368 Therefore, to draw some conclusive evidence about whether or not IAM.SPH phase complies with Adveef's
369 "pH piston hypothesis", we decided to compare affinity data achieved on either phase, *i.e.* IAM.PC and
370 IAM.SPH, exactly in the same analytical conditions and using 30% (v/v) methanol as organic modifier,
371 collected from (De Vrieze et al., 2014). The retention data are reported in Table S2, while graphs are shown
372 in Figure S2. This data shows that on the IAM.PC most bases are shifted upwards with regards to the
373 "neutrals" regression line (Figure S2a) – with only one base lying below. On the contrary, on the IAM.SPH
374 most bases are instead either overlapping the "neutrals" regression line or alternatively lying below it. The
375 acidic compounds are in both cases retained less than neutral isolipophilic molecules. However, the distance
376 from the regression line is clearly higher on the IAM.PC than on the IAM.SPH, suggesting that the electrostatic
377 repulsion is way stronger on the latter, even though the number of acids (*n* = 11) assayed is limited.

378 These findings all in all suggest that while neutrals interplay identically on both phases, when it comes to
379 ionizable compounds the selectivity of these IAM phases markedly changes. The presence of electronic

charges seems to disrupt the interaction in a more consistent way on the IAM.SPH than on IAM.PC, on which partitioning of basic compounds is enhanced. We can conclude that IAM.SPH does not conform to the "pH piston hypothesis" and the addition of acetonitrile 15% (v/v) produces a measurable effect on the partitioning of acids, which appears to be enhanced.

3.1.3 BR analysis

The four investigated datasets (Neutrals, Acids, Bases and Dataset) were submitted to BR analysis to deconvolute the balance of the intermolecular forces governing retention. The experimental procedure is described in the Materials and Methods Section. PLS statistics are in Table S3.

3.1.3.1 Neutral compounds

As previously mentioned, the same 36 neutral compounds assayed by Lombardo *et al.* (Lombardo et al., 2000)(dataset Neutrals) were firstly investigated. This choice was motivated by the aspect that this dataset features wide lipophilicity range (6 log $P^{n\text{-oct/water}}$ units) and has been extensively used to characterize different chromatographic systems by BR analysis (Ermondi and Caron, 2018). Therefore, assaying these compounds allows us to contrast and compare with *n*-octanol/water and IAM.PC partition systems (data in Table S4). Statistics show that, although the accuracy of models based on log $k^{IAM.SPH}$ is good (r^2 = 0.80 and q^2 = 0.60, Figure S3b), this is inferior to that of the other two models which performs slightly better.

BR plots of log $k^{IAM.SPH}$, log $P^{n\text{-oct/water}}$ and log $k_w^{IAM.PC}$ are compared in Figure 4. Absolute BR plots evidences that (*i*) retention on the IAM.PC phase is more affected by molecular size (green block) as compared to the other two systems; (*ii*) the solutes H-bond acceptor and donor properties (blue and red block, respectively) depicted by neutral compounds on the IAM.SPH resemble quite closely those of the *n*-octanol/water partition system; (*iii*) the polarity contribution (light blue block) between the two IAM phases is very similar and less important that encoded in the *n*-octanol/water partition system. The BR plots with sign highlights that, as expected because of the reverse nature of the system, the larger the compound the more retained, and the higher its interaction with water the less retained. Notably the capacity of solutes to act as hydrogen bond donor increases their interaction with the stationary phase in a more pronounced way when log $k^{IAM.SPH}$ is considered. Conversely, a compound which exhibit high hydrogen bond acceptor skills is penalized and thus poorly retained by the system.

Overall, retention on the IAM.SPH phase for neutral compounds seems to be led by a peculiar H-bonding pattern in comparison with the other systems. This could be due to the presence of the alcoholic hydroxy group in the IAM.SPH (Figure 1), which has indeed both H-bond acceptor and donor capabilities.

Finally, the evidence that the polarity contribution is very similar for both IAM phases and lower than that of log $P^{n\text{-oct/water}}$ could suggest that the free silanol groups and the silica itself do not play a significant role in retention and demonstrates that quality of column manufacture and that the synthesis itself is fully compliant to industrial standard. In fact, according to these data it seems that secondary, unintended interactions with the propyl amino moieties on the silica of the IAM.SPH, if occur, disrupt pure retention to an extent that is comparable to that of industrially produced IAM.PC columns.

3.1.3.2 Acids

PLS models produced by the Acids dataset shows solid statistics (r^2 = 0.76 and q^2 = 0.57,) with two LVs. The BR plot (Figure 5) with sign indicates that the blocks that affect retention by a larger extent are those related to molecular size and hydrophobicity. Such an involvement of hydrophobicity was not observed for neutral compounds. Moreover, H-bonding capabilities, as either donor or acceptor, seem to play a very minor role in driving the analytical retention for such compounds. This evidence could be in principle motivated by the aspect that the solutes that support hydrogens that are covalently bound to heteroatoms (mostly oxygens) or in general the acidic protons are released as a consequence of ionization and therefore cannot possibly act as H-bond donors. However, this would not explain why H-bond acceptor capability would not affect analytical retention as in pure principle, negatively charged heteroatoms should be more prone to establish H-bonding. The fact that the IAM.SPH measurements were conducted at relatively high ratio of organic modifier, *i.e.* 40% (v/v), lowering not only the difference in polarity between stationary phase and eluents but also the pKa of ionizable compounds, does not explain this outcome as for neutral compounds instead H-bonding was proved to impact IAM.SPH affinity. A reasonable explanation to this evidence can be retrieved in the concept of QSPR on which BR analysis is based. In fact, in a QSPR model a mathematical relationship is sought between the variation of the property and the variation in the descriptors. In the case of acidic compounds, the negative charge is present in all the substances and therefore it does not vary along the dataset. QSPR and thus BR analysis do not catch this information and therefore the interaction with the IAM.SPH is found to be due to the intermolecular interactions not related to the presence of the charge, size and hydrophobicity and the capacity of interacting with water (light blue block, detrimental for the interaction). This explanation is in line with what has been reported in a previous paper in which the BR analysis of IAM.PC has been performed (Ermondi et al., 2018).

3.1.3.3 Bases

PLS models produced by the Bases dataset (Table S3) are of poor statistical quality, even when paroxetine, which behaves as a strong oulier, is removed from the dataset. This finding makes unreliable the information content produced by BR analysis and thus no graphical output has been reported.

3.1.3.4 Dataset

In a final stage, the Dataset was submitted to BR analysis and no robut PLS model has been found. However, if the bases are excluded along with antipyrine (which behaved as outlier) a good accuracy (r^2 = 0.76 and q^2 = 0.60) is reached despite a smaller dataset (n = 61). These results are reported in Figure 6.

The BR plot of this dataset which includes neutral and negatively charged compounds supports that analytical retention is mostly driven by molecular size and hampered by polarity. While the net contribution of hydrophobicity seems negligible, analytical retention seems to be hindered by the tendency of molecules to accept H-bonding. This is reasonable if we look at the IAM.SPH structure (Figure 1 and graphical abstract), which supports H-bond acceptor moieties that are not present on the IAM.PC. Notably, the decrease of the relevance of the red block (solutes HBD) in comparison with Figure 4 (neutral compounds) when anionic structures are introduced in the dataset, support the detrimental effect of charges discussed in the previous section 3.1.2.

3.1.4 QSPR models

Since the statistics of the model related to the analytical retention of basic compounds were poor, we tried another *in silico* approach to improve the predictive strength of the models. The experimental details are described in 2.2.4. The neutrals, acids and bases datasets were modeled with three independent variables whereas for the Dataset four variables were set. The results are listed in Table 2, while statistical models that are normalized to fit the same scale to allow an unbiased comparison between descriptors are in Table S5. All the models are statistically validated, and for the sake of conciseness, only the models optimized through Leave-One-Out (LOO) crossvalidation runs are presented. A list of relevant descriptors is available in the supporting information (Table S6).

For Acids and Bases, the best results were achieved by assuming all the molecules in their charged forms, despite of the evidence that ionizable molecules are present in solution as a mixture of neutral and charged abundances that are function of their experimental pK_a. This is extremely consistent with the experimental evidence described in 3.1.2, as we noted that electrical charges, especially positive, has a disrupting effect on retention if compared with neutral compounds of equal lipophilicity. As listed in Table 2, for the Neutrals dataset a satisfactory statistic model is achieved (r^2 = 0.86). Retention of these compounds was found to be

directly related to molecular VirtualLogP and the number torsions and inversely related to Lipole (Mauri et al., 2017).

The models describing retention of acidic solutes also show remarkable statistics (although not as good as the that of the neutral compounds, with r^2 = 0.84 on a significantly lower number of solutes) and seems to be promoted for highly lipophilic (once again Virtual Log P – in this case calculated from the anionic forms) and bulky (Vdiam which stands for volume diameter) and hindered by molecular flexibility. These outcomes are consistent with the BR analysis detailed in 3.1.3.2.

From 3.1.3.3, we know that the modeling of the retention of bases on IAM.SPH phase based on BR analysis was problematic. However, when QSPR with different descriptors and algorithmis conducted, the statistics is still good (r^2 = 0.81) although the least accurate among the QSPR models so far presented. Retention of basic compound was found to be (again) directly related to VirtualLog P, lipole and number of rings. The analyte removed to maximize the predictive stength of the model – hydroxyzine – is the only basic compound of the dataset supporting two basic functions rather than only one. Therefore, the interplay between electric charges might have played a role, even though at the experimental pH 7.4, the solute should theoretically prevail in its monocationic form. Seven compounds, i.e. cimetidine, metoprolol propranolol, quinidine, ropinirole, tramadol and venlafaxine, despite having very similar affinity on IAM.SPH (from -0.616 to -0.640) have a predicted retention falling in a nearly one-unit range (from -0.801 to 0.005). These compounds are structurally unrelated therefore the substandard prediction for these cannot be motivated on specific structural features. Moreover, the datapoints seem to aggregate in two data clusters. This is also evident in Figure S4.

Finally, we assembled all the compounds in one dataset (Eq (5)) and ran the modeling with 4 dependent variables. The model achieved, as well as the previous ones (from Eq (2) to (4)) allows retention time prediction having solid statistics (r^2 = 0.74) and a quite high Fisher coefficient (59.30). The plots experimental *vs* predicted log $k^{IAM.SPH}$ values for the subsets (*a,b,c*) and for the complete dataset (*d*) are shown in Figure 7. A further validation is listed in Table S7.

3.2 Biological barrier permeability prediction

From the results so far achieved, the IAM.SPH demonstrated to exhibit some sort of originality when compared to IAM.PC on the market. However, the point that still needs clarification is whether this selectivity is relevant in drug development programs to reduce the attrition rates and direct efforts only on the most promising candidates, discontinuing the implementation of other molecules featuring substandard membrane permeability.

The previous work (De Vrieze et al., 2014) addresses partly this concern, as it was thereby demonstrated that the IAM.SPH proved as effective as IAM.PC and cholesteryl stationary phases in the prediction of log BB, *i.e.* the logarithm of the brain - to - plasma distribution ratio estimated *in vivo*. However, if on one hand optimizing CNS candidate selection based on the value of log BB is a well-established practice, on the other hand solid evidences (Hammarlund-Udenaes et al., 2008) suggest that when used in isolation, this can be a misleading parameter, since it is generally accepted that it is the unbound drug that exerts the pharmacological effect. Indeed, Summerfield and co-workers emphasized how increasing lipophilicity does not necessarily result in increased efficacy and may instead lead medicinal chemists astray in a chemical space that is hardly druggable due to poor solubility and metabolic instability. This approach might actually transpire to be one of the most misleading exercises within modern drug discovery (Jeffrey and Summerfield, 2007).

For this reason, we decided to consider *in vivo* BBB permeation parameters taken from the literature (Avdeef, 2012) other than log BBB, focusing specifically on brain and plasma unbound fractions.

The fraction unbound in plasma ($f_{u,p}$) seems to be at some extent inversely related to the retention coefficients achieved on the IAM.SPH phase (Figure 8a). Interestingly, this relationship is much weaker when data on IAM.PC extracted from the literature (Ermondi et al., 2018) are used (Figure S6). The fraction unbound in plasma is an important determinant of drug efficacy in pharmacokinetic and pharmacodynamic studies. This is because, in general, only the unbound (free) drug can interact with pharmacological target proteins such as receptors, channels, and enzymes and can diffuse between plasma and tissues. In *in vivo* BBB partitioning studies, the fraction unbound in plasma is an indication of the amount of compounds exposed to the CNS and that can be readily up taken by the brain. The capability to surrogate the values of fraction unbound in plasma is also extremely beneficial in the optimization of therapeutic dose. In fact, for drugs having large values of fraction unbound in plasma, smaller doses can be administered allowing a more selective action and a mitigation of untoward effects.

However, once reached the brain it is the unbound fraction to brain that is responsible of the pharmacological action; therefore an estimate of both $f_{u,pl}$ and fraction unbound in brain ($f_{u,br}$) would be desirable for a more successful brain delivery strategy.

To compare with a tool routinely employed by pharmaceutical enterprises and in an attempt to broaden our vision concerning the BBB partitioning of therapeutics, we selected from the literature (Tsinman et al., 2011) data achieved by parallel artificial membrane permeability assay (PAMPA) BBB. Indeed, PAMPA, developed by Kansy and co-workers (Kansy et al., 1998), is a non-cell-based, high-throughput permeation model which is widely used in the early phase of drug discovery for the prediction of passive diffusion of drug molecules across phospholipid membranes. Different implementations of this techniques have been developed in

recent years to mirror the specific compositions of the barriers under study, with the PAMPA BBB adapted to study the diffusion of therapeutics through the BBB. This is based on the stratification of a porcine brain lipid extract (PBLE) based artificial membrane dissolved in *n*-dodecane. The *in vivo* and *in vitro* data is reported in Table 3. Please note that PAMPA BBB P_0 measurements refer to the permeability ($cm \cdot s^{-1}$)—of the neutral species only, whereas PAMPA BBB P_M determinations reflect PAMPA transmembrane permeability (which is P_e, i.e. PAMPA effective permeability coefficient ($cm \cdot s^{-1}$)—the experimentally-determined value) corrected for the permeability of the aqueous boundary layer and aqueous pore diffusion effects. PAMPA BBB P_M 7.4 are values adjusted at physiological pH according to the Henderson-Hasselbalch equation.

Interestingly, the fraction unbound to brain seems to be well-parameterized by PAMPA BBB P_M 7.4 (Figure 8b). Interestingly, no relationship was observed between retention data on both IAM phases and PAMPA BBB P_0 measurements. This was not at all surprising as most PBLE formulations available of the market feature a content of PC below 13 % and an unknown concentration of SPH.

All in all these results suggest that IAM.SPH LC has a good potential to be implemented in drug development programs as it proved effective in the estimation of both log BB and of the $f_{u,pl}$.

4. Concluding remarks

The IAM.PC stationary phases currently available of the market present several shortcomings, the most important being their lack in accuracy in representing some of the lipids structuring strategic body districts. The BBB is made of SPH for over 33% (v/v), making up for the most abundant lipid in this biological barrier which represents the obstacle that more than others jeopardizes the efforts of pharma companies aiming to produce drugs targeting the brain. Although an IAM phase based on SPH is not commercially available to date, a prototype was realized by the Separation Science Group in 2011 (Verzele et al., 2012) and used for drug partitioning studies (De Vrieze et al., 2014). However, a deep characterization of analytical retention on this stationary phase was not so far envisaged. This was fulfilled by the present work, which clearly demonstrates that:

1. Although retention of neutral compounds is similarly dependent on *n*-octanol/water lipophilicity, the IAM.SPH retains originality when affinity for solutes supporting ionizable moieties is measured;
2. On the basis of the data collected, IAM.SPH does not comply to the Avdeef's "pH piston hypothesis" (Avdeef et al., 1998) but rather reverts it;
3. BR analysis proved, especially for neutral and acidic compounds, a valuable tool to scrutinize and visually represent and interpret the intermolecular forces governing retention on this novel phase;

4. QSPR modeling allowed prediction of retentive behavior usable for instance in virtual screening scenarios. In these settings, in fact, if some minor accuracy loss might be a reasonable price to pay for much faster estimates;
5. The IAM.SPH demonstrated relevant not only in prediction of log BB as already evidenced (De Vrieze et al., 2014) but also in the estimation of a drug's fraction unbound in plasma, a parameter that is crucial not only in BBB permeation but also in drug delivery and therapeutic dose optimization.

Both BR analysis and QSPR can be run in batch, the former in MatLab and the second in VEGA ZZ 64 interfaces, and on mid-range CPUs hence meeting the demands of private users and smaller enterprises.

579 **Tables**

580 **Table 1.**

Chemical	log $k^{IAM.SPH}$	log $P^{n\text{-oct/water}}$	pKa	Chemical nature	Supplier
3,5- dichlorophenol	1.027	3.68		N	Merck
3- bromoquinoline	0.459	3.03		N	Merck
3- chlorophenol	0.412	2.50		N	Merck
4- aminobenzoic acid	-1.795	0.83	4.62	A	Acros Organics
acetaminophen	-0.794	0.51		N	Acros Organics
acetophenone	-0.243	1.58		N	Merck
acetylsalicylic acid	-1.269	1.18	3.50	A	Acros Organics
allopurinol	-1.417	-0.55		N	Merck
amitriptyline	0.539	4.92	9.17	B	TCI Europe
amobarbital	0.014	2.07	7.48/11.15	A	Merck
antipyrine	-1.002	0.38		N	Acros Organics
atenolol	-1.620	0.16	9.19	B	Acros Organics
atorvastatin	0.768	6.36	4.46	A	Merck
bifonazole	1.488	4.77		N	Merck
bromazepam	-0.101	1.65		N	Merck
caffeic acid	-0.719	1.15	4.62	A	Acros Organics
caffeine	-1.335	-0.07		N	Acros Organics
carbamazepine	0.012	2.19		N	Acros Organics
celecoxib	1.157	3.53	9.38	A	Acros Organics
chlorambucil	0.811	3.90	4.60	A	TCI Europe
chloramphenicol	-0.014	1.14		N	Acros Organics
chlorpromazine	0.891	5.41	9.50	B	TCI Europe
cimetidine	-0.627	0.40	7.01	B	TCI Europe
citalopram	0.142	3.76	9.22	B	TCI Europe
clotrimazole	1.336	5.20		N	Acros Organics
cyclobenzaprine	0.518	5.20	8.47	B	TCI Europe
desipramine	0.516	4.90	10.28	B	Merck
dexamethasone	-0.026	1.83		N	Acros Organics
diazepam	0.520	2.79		N	Cerilliant
diclofenac	0.791	4.51	3.99	A	Acros Organics
diethylstilboestrol	1.672	5.07		N	Merck

domperidone	0.531	3.90	9.68	B	TCI Europe
donepezil	0.000	4.70	8.54	B	Acros Organics
estradiol	1.228	4.01		N	Merck
ethosuximide	-1.004	0.38	9.27	A	Acros Organics
fexofenadine	0.091	2.81	7.84	A	Merck
fluconazole	-0.820	0.50		N	Merck
flurbiprofen	0.482	4.16	4.18	A	Acros Organics
furosemide	-0.109	2.06	9.90	A	Acros Organics
gallic acid	-1.484	0.70	8.54	A	Acros Organics
griseofulvin	0.240	2.18		N	Acros Organics
hexobarbital	-0.154	1.98	8.20	A	Merck
hydrochlorothiazide	-0.351	-0.07	9.80	A	Merck
hydrocortisone	0.100	1.55		N	Acros Organics
hydrocortisone 21- acetate	0.375	2.19		N	Merck
hydroxyzine	-0.635	3.43	7.52/1.58	B	Merck
ibuprofen	0.433	3.97	4.24	A	Acros Organics
imipramine	0.458	4.80	9.52	B	Acros Organics
ketoprofen	0.032	3.12	4.00	A	TCI Europe
ketorolac	-0.222	2.10	3.84	A	TCI Europe
lorazepam	0.399	2.51		N	Cerilliant
lormetazepam	0.362	2.72		N	Cerilliant
methylthioinosine	-0.817	0.09		N	Aurora
metoclopramide	-0.433	2.67	9.71	B	TCI Europe
metoprolol	-0.603	2.15	9.56	B	TCI Europe
metronidazole	-1.153	-0.02		N	Acros Organics
naphthalene	0.767	3.37		N	Acros Organics
naproxen	0.104	3.18	4.14	A	Acros Organics
nifedipine	0.463	3.17		N	Acros Organics
nifuroxime	-0.092	1.28		N	Merck
nitrofurazone	-0.546	0.23		N	TCI Europe
nortriptyline	0.606	3.90	10.13	B	TCI Europe
paroxetine	0.641	2.53	9.77	B	TCI Europe
pentobarbital	0.043	2.10	8.18	A	Cerilliant
pentoxifylline	-0.966	0.29		N	TCI Europe
phenobarbital	-0.211	1.47	7.41	A	Cerilliant

phenytoin	0.344	2.47	8.28	A	Merck
piroxicam	0.008	3.06	5.29	A	TCI Europe
prednisolone	0.119	1.60		N	TCI Europe
prednisone	-0.078	1.46		N	TCI Europe
promethazine	0.597	4.81	9.00	B	TCI Europe
propranolol	-0.635	3.48	9.16	B	Acros Organics
quinidine	-0.618	3.44	8.56	B	Acros Organics
quinoline	-0.145	2.03		N	TCI Europe
ranitidine	-1.194	0.20	8.33	B	TCI Europe
rifampicin	0.591	2.70	1.70	B	TCI Europe
ropinirole	-0.640	3.06	10.17	B	Merck
salicylic acid	-0.361	2.26	2.82	A	Acros Organics
terbutaline	-0.885	0.90	11.02	B	Cerilliant
testosterone	0.727	3.29		N	Cerilliant
thiamphenicol	-0.770	-0.27		N	Acros Organics
tolnaftate	1.928	5.40		N	TCI Europe
tramadol	-0.608	1.34	9.41	B	Merck
triprolidine	-0.027	3.92	8.64	B	Merck
valproic acid	-0.321	2.75	4.54	A	Acros Organics
venlafaxine	-0.616	2.69	9.67	B	Acros Organics
verapamil	0.212	3.69	8.68	B	Acros Organics
warfarin	0.066	2.70	4.82	A	TCI Europe

Table 1. Common names, logarithms of the chromatographic retention coefficients on the IAM.SPH stationary phase, pKa values, chemical nature (A = acids, B = bases and N= neutral compounds) and suppliers for the 88 compounds measured in the present study.

Table 2.

Dataset	Variables	*N*	r^2	SE	F	ExRow	Equation	Eq (n)
neutrals	3	35	0.86	0.336	61.52	3,5-dichlorophenol	-1.5401 + 0.4195 VirtualLogP + 0.0606 Torsions - 0.0517 Lipole	2
acids	3	25	0.84	0.307	37.14	fexofenadine	-3.6851 + 0.3963 VirtualLogP + 0.4457 Vdiam - 0.1443 FlexTorsions	3
bases	3	25	0.81	0.319	29.56	hydroxyzine	-1.7191 + 0.2806 Rings + 0.1946 VirtualLogP + 0.3215 Lipole	4
dataset	4	87	0.74	0.396	59.30	fexofenadine	-1.9477 + 0.3391 VirtualLogP + 0.1953 Rings + 0.0890 Lipole + 0.1052 Vdiam	5

Table 2. Statistic models based on QSPR analysis along with validation for various compound classes.

606 **Table 3**

607

Name	$f_{u,pl}$ (Avdeef, 2012)	$f_{u,br}$ (Avdeef, 2012)	$f_{u,pl}/f_{u,br}$ (Avdeef, 2012)	PS (Avdeef, 2012)	$t_{1/2}$ (min) (Avdeef, 2012)	PAMPA BBB log P_0 (Tsinman et al., 2011)	PAMPA BBB log P_m 7.4 (Tsinman et al., 2011)
acetaminophen	0.744	0.807	0.925	38.000	3		
amitriptyline	0.090	0.003	28.000	1414.000	9	-1.27	435
caffeine	1.045	0.810	1.550	165.000	1.5	-5.92	1
carbamazepine	0.258	0.118	2.267	401.0	3		
celecoxib	0.001	0.003	0.300	207.0	25		
chlorpromazine	0.035	0.001	47.000	774.0	28	-1.46	496
cimetidine	0.810	0.530	1.500	3.7	15	-6.40	0.40
citalopram	0.226	0.043	5.667	89.3	11	-2.09	99
cyclobenzaprine	0.054	0.007	7.000	1905.0	5		
dexamethasone	0.272	0.098	3.000	31.0	12		
diazepam	0.109	0.053	2.050	370.0	4	-3.83	148
diclofenac	0.012	0.055	0.200	58.0	11		
donepezil	0.285	0.102	3.000	200.0	4		
ethosuximide	0.815	0.742	1.100	34.0	4	-5.83	1.50
fexofenadine	0.350	0.077	5.000	0.4	136	-5.17	5
flurbiprofen	0.006	0.129	0.050	160.0	4	-2.35	3
hydroxyzine	0.052	0.010	5.000	417.0	10	-3.72	82
ibuprofen	0.016	0.296	0.100	93.0	4	-2.64	4
ketorolac	0.058	0.485	0.100	1.7	23		
metoclopramide	0.710	0.310	2.300	21.0	8	-1.11	380
metoprolol	0.900	0.183	5.000	18.0			
naproxen	0.018	0.542	0.030	68.0	3	-2.63	0.60

nortriptyline	0.031	0.005	7.000	314.0	17		
paroxetine	0.015	0.004	4.000	21.0	80		
phenytoin	0.161	0.104	1.733	64.0	8	-4.34	41
propranolol	0.120	0.022	7.500	770.0	6	-1.93	87
quinidine	0.160	0.037	4.000	21.0	24	-2.85	93
ranitidine	0.960	0.960	1.000	0.5	31		
rifampicin	0.120	0.140	0.900	0.1			
salicylic acid	0.280	1.064	0.300	4.0	10	-3.34	0.02
tramadol	0.850	0.234	4.000	4.3			
triprolidine	0.310	0.092	3.000	501.0	3		
venlafaxine	0.648	0.215	3.033	104.0	4		
verapamil	0.115	0.026	4.500	255.0	8	-2.03	196

Figures

Figure 1

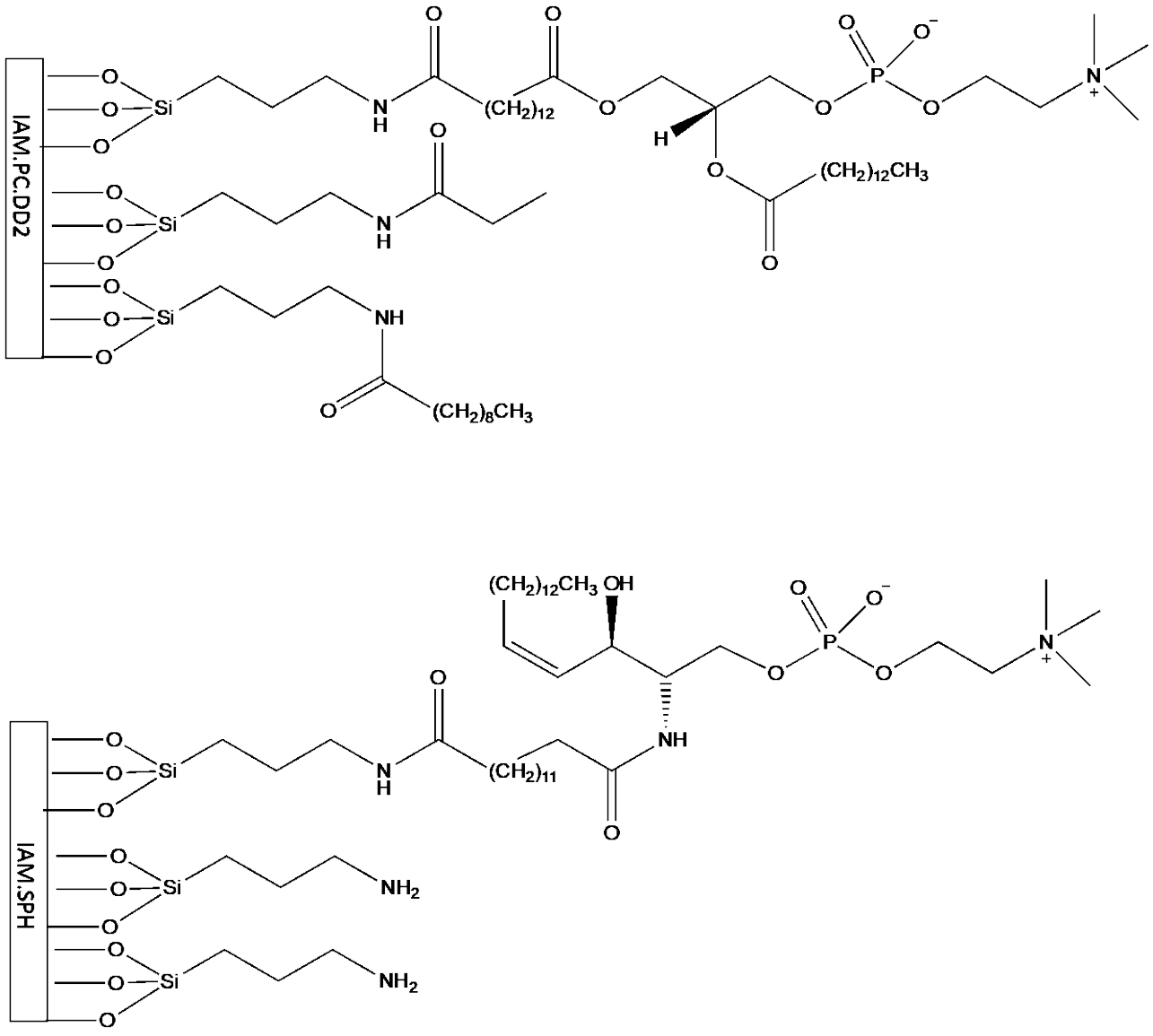

Figure 1. Chemical structure of the industrially immobilized artificial membrane phase IAM.PC and of the in house synthetized IAM.SPH prototype. Free silanol groups – although present – are not displayed.

635 **Figure 2**.

a.

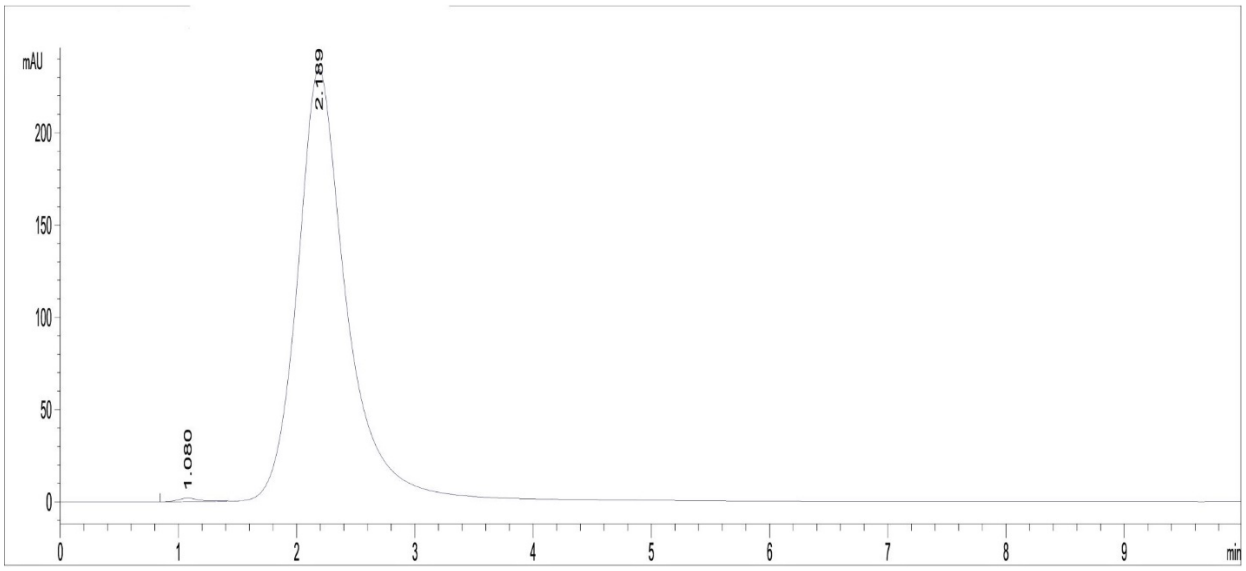

b.

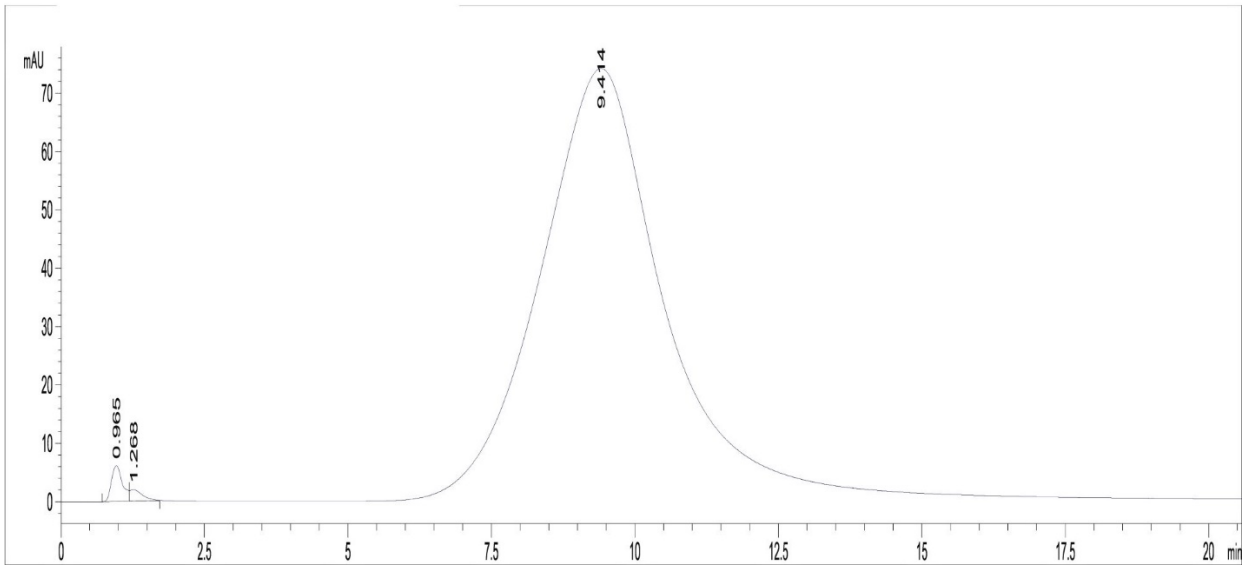

636

637

638 **Figure 2**. UV chromatograms of donepezil (*a*) and chlorpromazine (*b*) measured in the present study. The
639 experimental conditions are described in 2.1.6, while the equipment used is detailed in 2.1.5.

640 **Figure 3.**

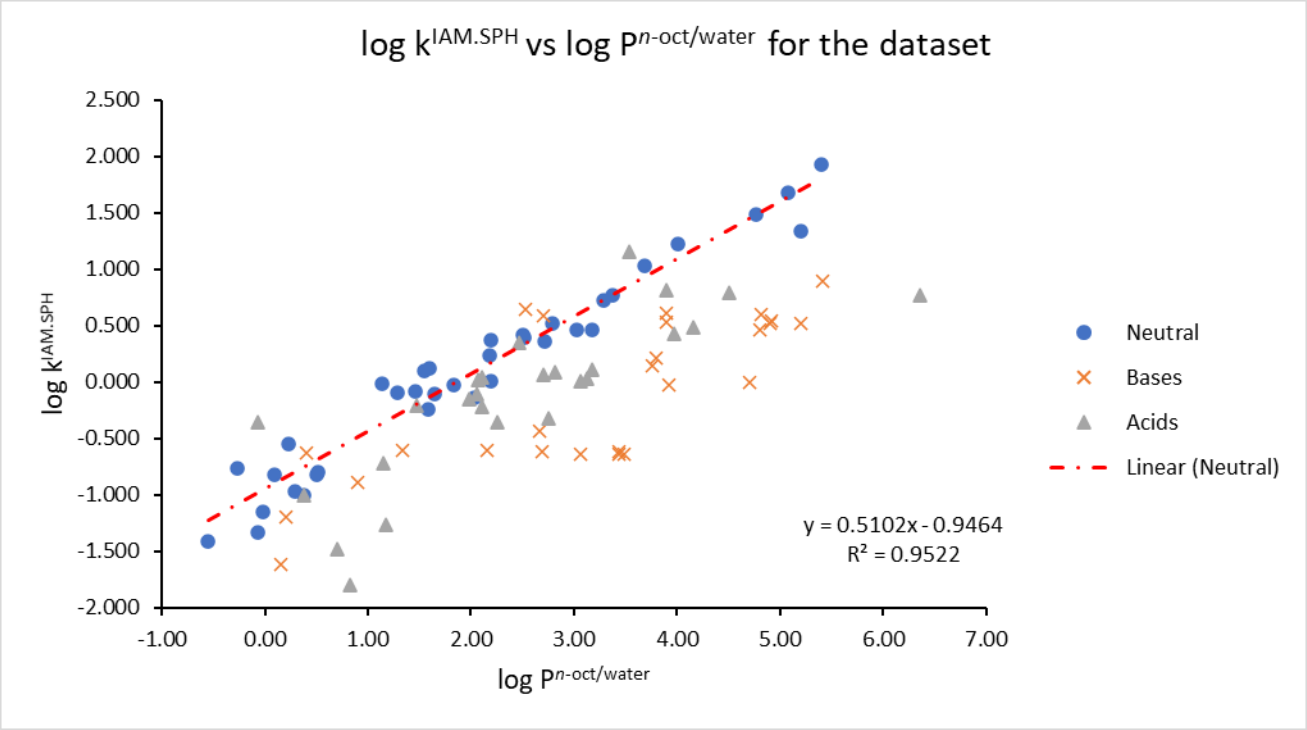

641

642

643 **Figure 3.** Graph plotting $k^{IAM.SPH}$ *vs* log $P^{n\text{-oct/water}}$ values for the complete dataset.

644

645

646

647

648

649

650

651

652

653

654

655

Figure 4.

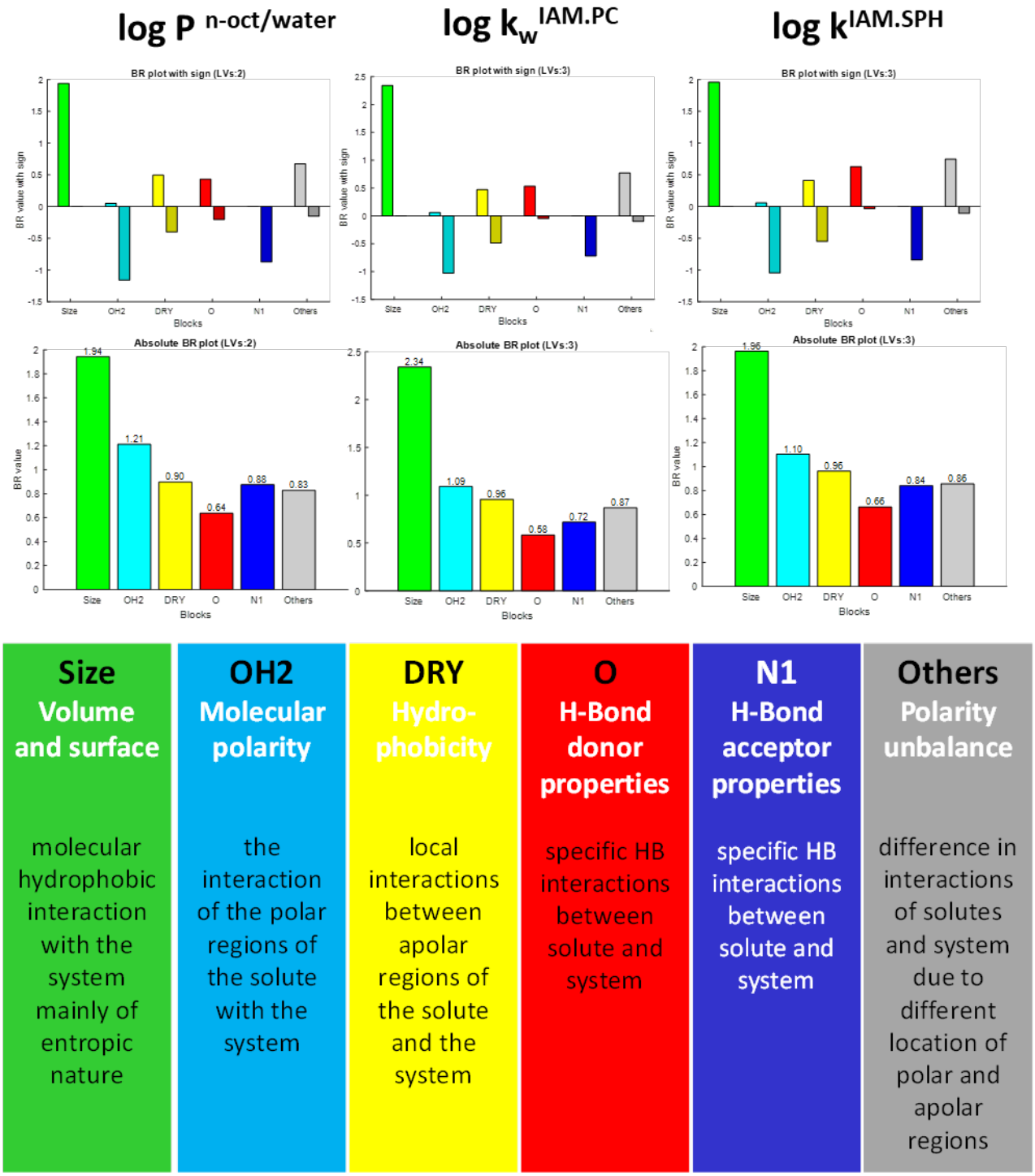

Figure 4. *On top,* comparison of the BR plots with sign and absolute BR plots for the 36 neutral compounds achieved for *n*-octanol/water partitioning and analytical retention on IAM.PC and IAM.SPH stationary phases. *At bottom*, a short explanation about the meaning of each block.

663 **Figure 5.**

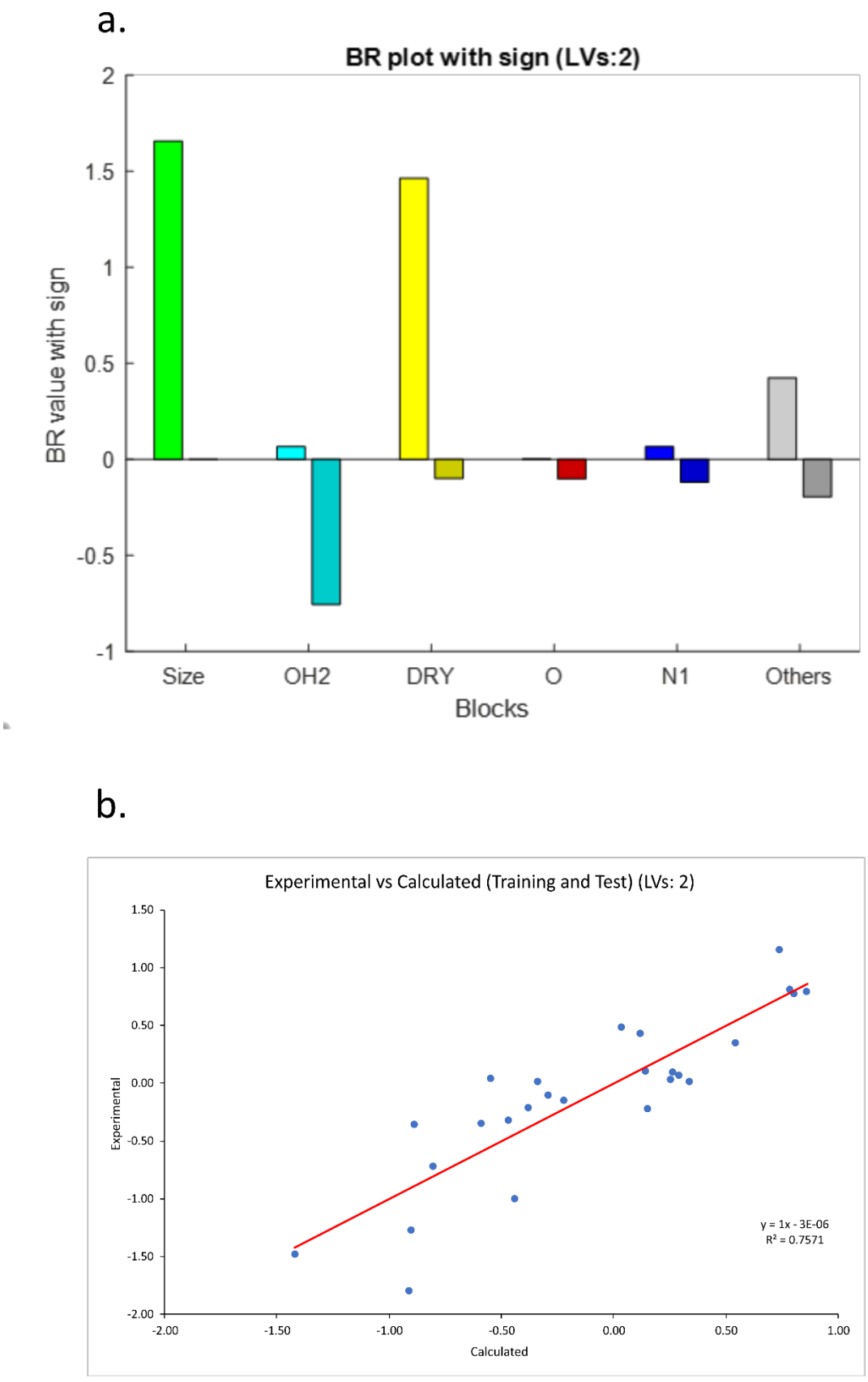

664

665 **Figure 5.** (*a*) BR plots with sign deconvoluting the interactions underlying the analytical retention on IAM.SPH

666 stationary phase and (*b*) plot experimental vs calculated log $k^{IAM.SPH}$ for the 26 acidic compounds.

Figure 6.

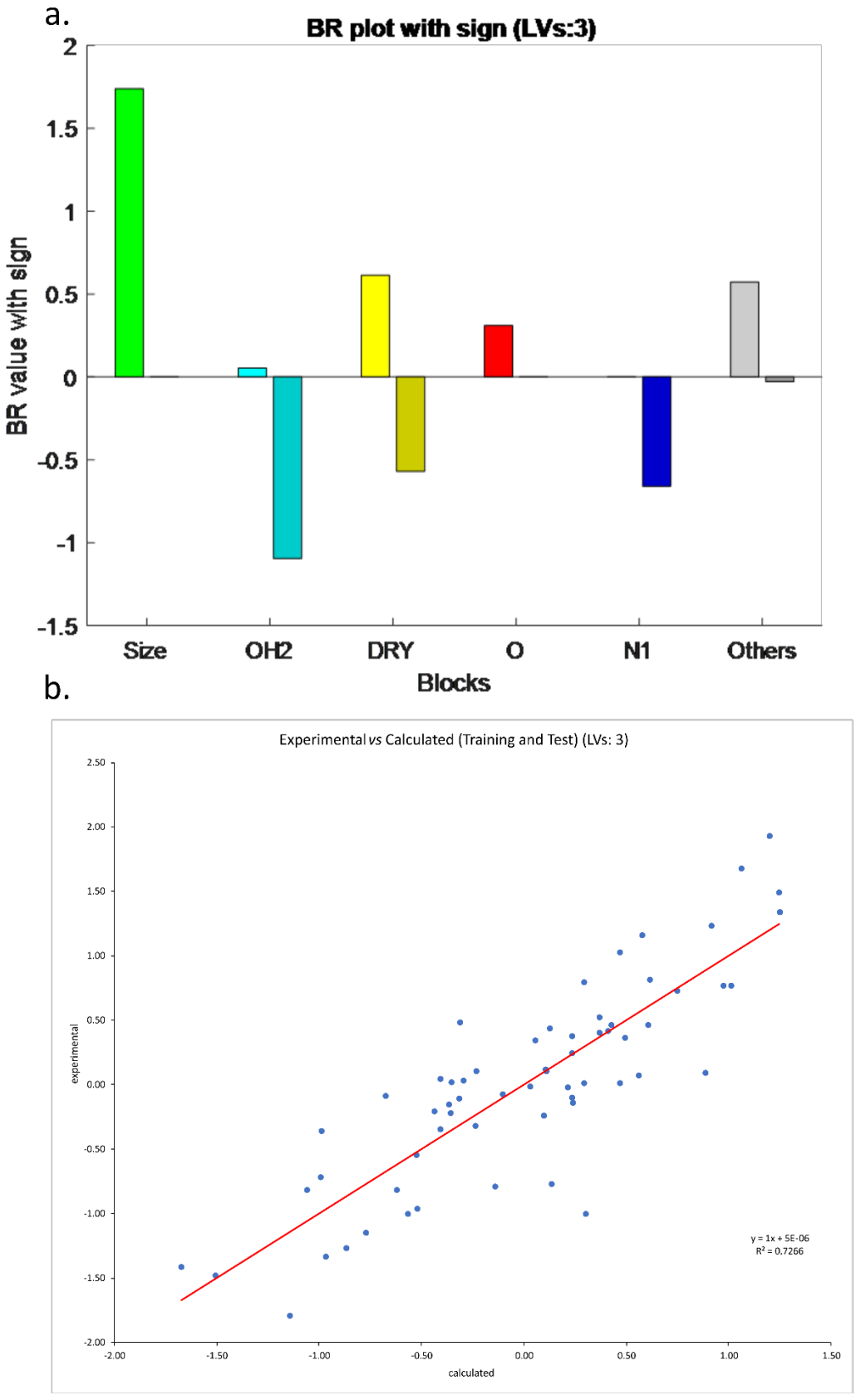

Figure 6. Plot experimental vs calculated log $k^{IAM.SPH}$ for the whole dataset. The outliers are mentioned at the top left.

Figure 7.

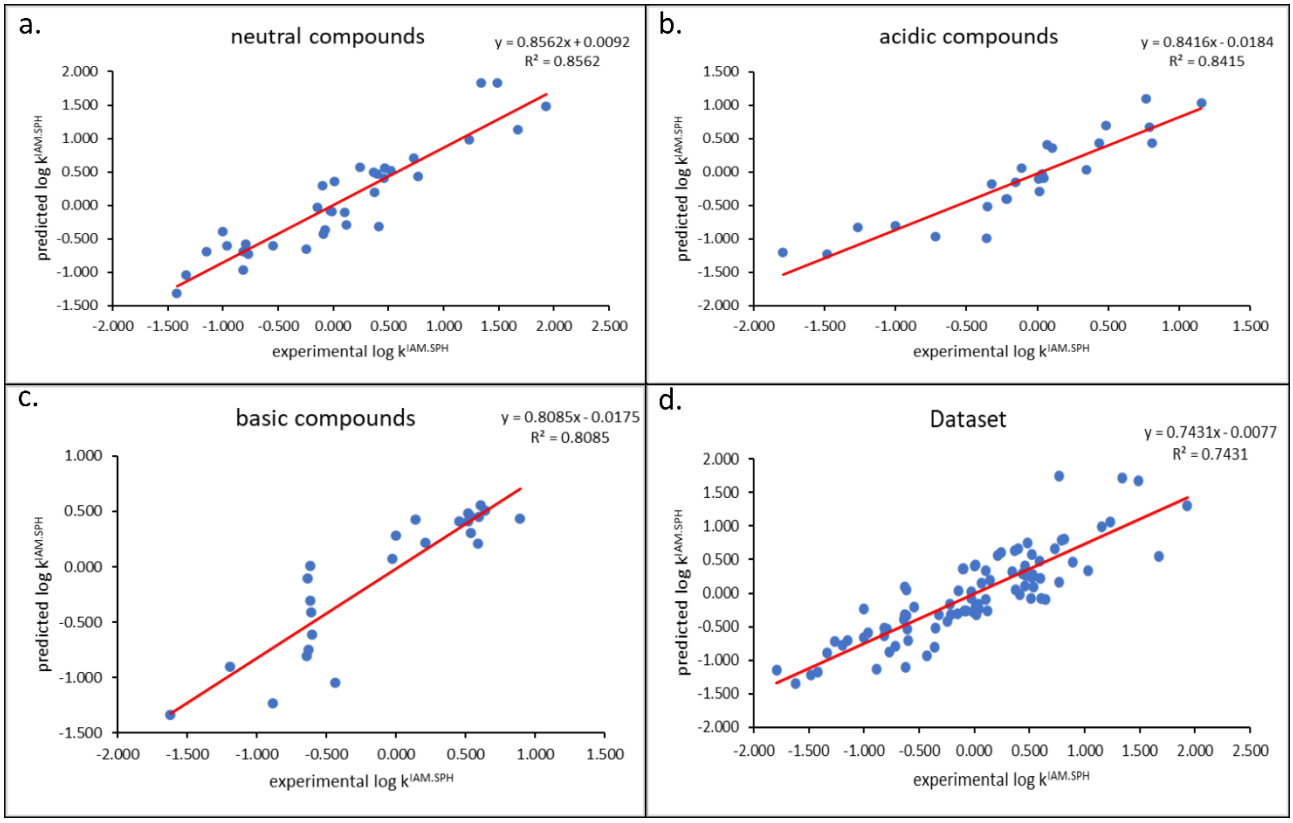

Figure 7. QSPR modeling: experimental vs predicted log $k^{IAM.SPH}$ plots for neutral (*a*), acidic (*b*), basic compounds (*c*) and for the whole dataset considered (*d*).

686 **Figure 8.**

a

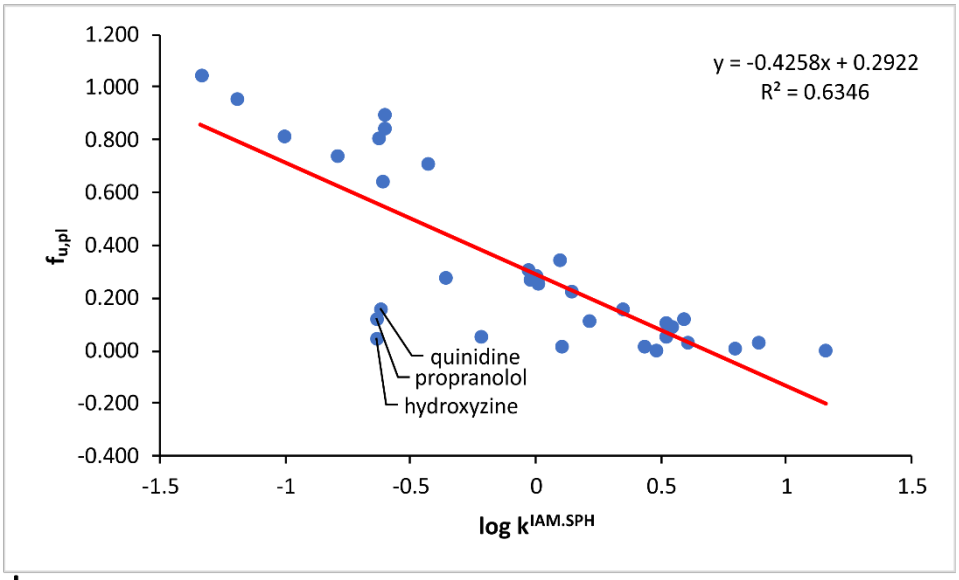

b

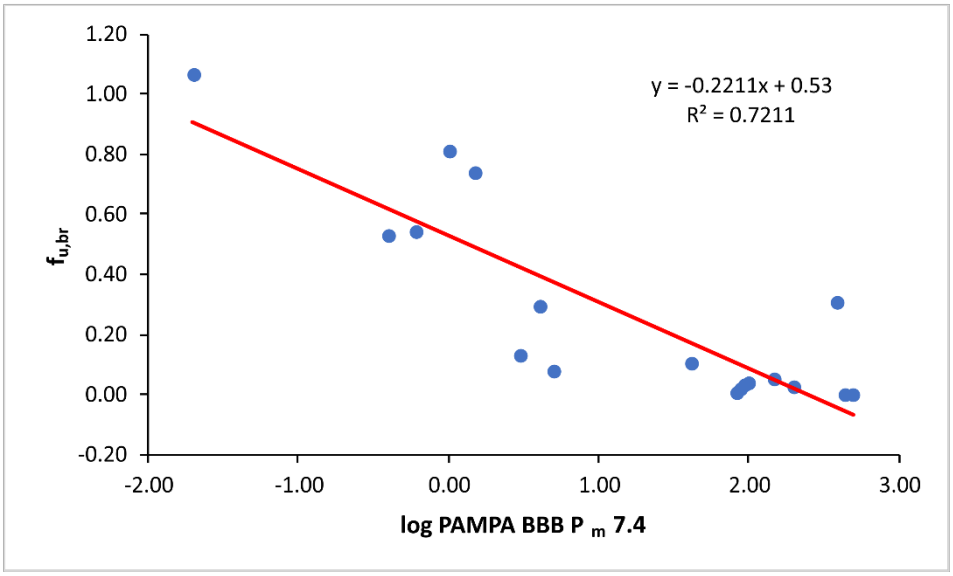

687

688 **Figure 8.** Logarithm of chromatographic retention coefficients measured on the IAM.SPH vs unbound fraction
689 in plasma. The three compounds deviating the most from the regression line are indicated.

690 **References**

691 Avdeef, A., 2012. Permeability: Blood-Brain Barrier, in: Sons, J.W. (Ed.), Absorption and Drug Development
692 Hoboken, NJ, USA pp. 625-663.
693 Avdeef, A., Box, K.J., Comer, J.E., Hibbert, C., Tam, K.Y., 1998. pH-metric logP 10. Determination of liposomal
694 membrane-water partition coefficients of ionizable drugs. Pharm Res 15, 209-215.
695 Bieberich, E., 2018. Sphingolipids and lipid rafts: Novel concepts and methods of analysis. Chem Phys Lipids
696 216, 114-131.
697 Braumann, T., Weber, G., Grimme, L.H., 1983. Quantitative structure—activity relationships for herbicides:
698 Reversed-phase liquid chromatographic retention parameter, log kw, versus liquid-liquid partition coefficient
699 as a model of the hydrophobicity of phenylureas, s-triazines and phenoxycarbonic acid derivatives. Journal
700 of Chromatography A 261, 329-343.
701 Brooks, B.R., Brooks, C.L., 3rd, Mackerell, A.D., Jr., Nilsson, L., Petrella, R.J., Roux, B., Won, Y., Archontis, G.,
702 Bartels, C., Boresch, S., Caflisch, A., Caves, L., Cui, Q., Dinner, A.R., Feig, M., Fischer, S., Gao, J., Hodoscek, M.,
703 Im, W., Kuczera, K., Lazaridis, T., Ma, J., Ovchinnikov, V., Paci, E., Pastor, R.W., Post, C.B., Pu, J.Z., Schaefer,
704 M., Tidor, B., Venable, R.M., Woodcock, H.L., Wu, X., Yang, W., York, D.M., Karplus, M., 2009. CHARMM: the
705 biomolecular simulation program. J Comput Chem 30, 1545-1614.
706 Brooks, B.R., Bruccoleri, R.E., Olafson, B.D., States, D.J., Swaminathan, S., Karplus, M., 1983. CHARMM: A
707 program for macromolecular energy, minimization, and dynamics calculations. Journal of Computational
708 Chemistry 4, 187-217.
709 Campbell, S.D., Regina, K.J., Kharasch, E.D., 2014. Significance of lipid composition in a blood-brain barrier-
710 mimetic PAMPA assay. J Biomol Screen 19, 437-444.
711 Cannon, R.E., Peart, J.C., Hawkins, B.T., Campos, C.R., Miller, D.S., 2012. Targeting blood-brain barrier
712 sphingolipid signaling reduces basal P-glycoprotein activity and improves drug delivery to the brain. Proc Natl
713 Acad Sci U S A 109, 15930-15935.
714 De Vrieze, M., Verzele, D., Szucs, R., Sandra, P., Lynen, F., 2014. Evaluation of sphingomyelin, cholester, and
715 phosphatidylcholine-based immobilized artificial membrane liquid chromatography to predict drug
716 penetration across the blood-brain barrier. Anal Bioanal Chem 406, 6179-6188.
717 Ducarme, A.N., M; Goldstein, S.; Massingham, R. , 1997. IAM retention and blood brain barrier penetration
718 Eur J Med Chem 33, 215-223.
719 Ermondi, G., Caron, G., 2012. Molecular interaction fields based descriptors to interpret and compare
720 chromatographic indexes. J Chromatogr A 1252, 84-89.
721 Ermondi, G., Caron, G., 2018. Block relevance (BR) analysis and polarity descriptors in property-based drug
722 design. ADMET and DMPK 6.
723 Ermondi, G., Caron, G., 2019. MLR, PLSR-BR Analysis and MBPLSR to Interpret Multivariate QSPR Models. The
724 Case of a Micellar Liquid Chromatography Descriptor (log KWSDS). Molecular Informatics 38, 1800144.
725 Ermondi, G., Vallaro, M., Caron, G., 2018. Learning how to use IAM chromatography for predicting
726 permeability. Eur J Pharm Sci 114, 385-390.
727 Ermondi, G., Visconti, A., Esposito, R., Caron, G., 2014. The Block Relevance (BR) analysis supports the
728 dominating effect of solutes hydrogen bond acidity on DeltalogP(oct-tol). Eur J Pharm Sci 53, 50-54.
729 Gaillard, P., Carrupt, P.A., Testa, B., Boudon, A., 1994. Molecular lipophilicity potential, a tool in 3D QSAR:
730 method and applications. J Comput Aided Mol Des 8, 83-96.
731 Garcia-Arribas, A.B., Alonso, A., Goni, F.M., 2016. Cholesterol interactions with ceramide and sphingomyelin.
732 Chem Phys Lipids 199, 26-34.
733 Gasteiger, J., Marsili, M., 1980. Iterative partial equalization of orbital electronegativity—a rapid access to
734 atomic charges. Tetrahedron 36, 3219-3228.
735 Goetz, G.H., Shalaeva, M., Caron, G., Ermondi, G., Philippe, L., 2017. Relationship between Passive
736 Permeability and Molecular Polarity Using Block Relevance Analysis. Molecular Pharmaceutics 14, 386-393.
737 Grumetto, L., Russo, G., Barbato, F., 2014. Indexes of polar interactions between ionizable drugs and
738 membrane phospholipids measured by IAM-HPLC: their relationships with data of Blood-Brain Barrier
739 passage. Eur J Pharm Sci 65, 139-146.

Grumetto, L., Russo, G., Barbato, F., 2015. Relationships between human intestinal absorption and polar interactions drug/phospholipids estimated by IAM-HPLC. Int J Pharm 489, 186-194.
Grumetto, L., Russo, G., Barbato, F., 2016a. Immobilized Artificial Membrane HPLC Derived Parameters vs PAMPA-BBB Data in Estimating in Situ Measured Blood-Brain Barrier Permeation of Drugs. Mol Pharm 13, 2808-2816.
Grumetto, L., Russo, G., Barbato, F., 2016b. Polar interactions drug/phospholipids estimated by IAM-HPLC vs cultured cell line passage data: Their relationships and comparison of their effectiveness in predicting drug human intestinal absorption. Int J Pharm 500, 275-290.
Hammarlund-Udenaes, M., Friden, M., Syvanen, S., Gupta, A., 2008. On the rate and extent of drug delivery to the brain. Pharm Res 25, 1737-1750.
Harrison, R.W., 1993. Stiffness and energy conservation in molecular dynamics: An improved integrator. Journal of Computational Chemistry 14, 1112-1122.
Jeffrey, P., Summerfield, S.G., 2007. Challenges for blood-brain barrier (BBB) screening. Xenobiotica 37, 1135-1151.
Kansy, M., Senner, F., Gubernator, K., 1998. Physicochemical high throughput screening: parallel artificial membrane permeation assay in the description of passive absorption processes. J Med Chem 41, 1007-1010.
Kim, S., Chen, J., Cheng, T., Gindulyte, A., He, J., He, S., Li, Q., Shoemaker, B.A., Thiessen, P.A., Yu, B., Zaslavsky, L., Zhang, J., Bolton, E.E., 2019. PubChem 2019 update: improved access to chemical data. Nucleic Acids Res 47, D1102-D1109.
Kim, S., Thiessen, P.A., Bolton, E.E., Chen, J., Fu, G., Gindulyte, A., Han, L., He, J., He, S., Shoemaker, B.A., Wang, J., Yu, B., Zhang, J., Bryant, S.H., 2016. PubChem Substance and Compound databases. Nucleic Acids Res 44, D1202-1213.
Kinoshita, M., Suzuki, K.G.N., Murata, M., Matsumori, N., 2018. Evidence of lipid rafts based on the partition and dynamic behavior of sphingomyelins. Chem Phys Lipids 215, 84-95.
Lombardo, F., Shalaeva, M.Y., Tupper, K.A., Gao, F., Abraham, M.H., 2000. ElogPoct: a tool for lipophilicity determination in drug discovery. J Med Chem 43, 2922-2928.
MacKerell, A.D., Brooks, B., Brooks, C.L., Nilsson, L., Roux, B., Won, Y., Karplus, M., 2002. CHARMM: The Energy Function and Its Parameterization, Encyclopedia of Computational Chemistry. John Wiley & Sons, Ltd.
Marakovic, N., Sinko, G., 2017. The Lock is the Key: Development of Novel Drugs through Receptor Based Combinatorial Chemistry. Acta Chim Slov 64, 15-39.
Mauri, A., Consonni, V., Todeschini, R., 2017. Molecular Descriptors, in: Leszczynski, J., Kaczmarek-Kedziera, A., Puzyn, T., G. Papadopoulos, M., Reis, H., K. Shukla, M. (Eds.), Handbook of Computational Chemistry. Springer International Publishing, Cham, pp. 2065-2093.
Natalini, B., Sardella, R., Camaioni, E., Macchiarulo, A., Gioiello, A., Carbone, G., Pellicciari, R., 2009. Derived chromatographic indices as effective tools to study the self-aggregation process of bile acids. J Pharm Biomed Anal 50, 613-621.
Ong, S., Liu, H., Pidgeon, C., 1996. Immobilized-artificial-membrane chromatography: measurements of membrane partition coefficient and predicting drug membrane permeability. J Chromatogr A 728, 113-128.
Pandey, P.K., Sharma, A.K., Gupta, U., 2016. Blood brain barrier: An overview on strategies in drug delivery, realistic in vitro modeling and in vivo live tracking. Tissue Barriers 4, e1129476.
Pedretti, A., Villa, L., Vistoli, G., 2002. Modeling of binding modes and inhibition mechanism of some natural ligands of farnesyl transferase using molecular docking. J Med Chem 45, 1460-1465.
Pedretti, A., Villa, L., Vistoli, G., 2004. VEGA--an open platform to develop chemo-bio-informatics applications, using plug-in architecture and script programming. J Comput Aided Mol Des 18, 167-173.
Pidgeon, C., Ong, S., Liu, H., Qiu, X., Pidgeon, M., Dantzig, A.H., Munroe, J., Hornback, W.J., Kasher, J.S., Glunz, L., et al., 1995. IAM chromatography: an in vitro screen for predicting drug membrane permeability. J Med Chem 38, 590-594.
Pidgeon, C., Stevens, J., Otto, S., Jefcoate, C., Marcus, C., 1991. Immobilized artificial membrane chromatography: rapid purification of functional membrane proteins. Anal Biochem 194, 163-173.
Pidgeon, C., Venkataram, U.V., 1989. Immobilized artificial membrane chromatography: supports composed of membrane lipids. Anal Biochem 176, 36-47.

Rossini, E., Bochevarov, A.D., Knapp, E.W., 2018. Empirical Conversion of pK a Values between Different Solvents and Interpretation of the Parameters: Application to Water, Acetonitrile, Dimethyl Sulfoxide, and Methanol. ACS Omega 3, 1653-1662.

Russo, G., Grumetto, L., Barbato, F., Vistoli, G., Pedretti, A., 2017a. Prediction and mechanism elucidation of analyte retention on phospholipid stationary phases (IAM-HPLC) by in silico calculated physico-chemical descriptors. Eur J Pharm Sci 99, 173-184.

Russo, G., Grumetto, L., Szucs, R., Barbato, F., Lynen, F., 2017b. Determination of in Vitro and in Silico Indexes for the Modeling of Blood-Brain Barrier Partitioning of Drugs via Micellar and Immobilized Artificial Membrane Liquid Chromatography. J Med Chem 60, 3739-3754.

Russo, G., Grumetto, L., Szucs, R., Barbato, F., Lynen, F., 2018. Screening therapeutics according to their uptake across the blood-brain barrier: A high throughput method based on immobilized artificial membrane liquid chromatography-diode-array-detection coupled to electrospray-time-of-flight mass spectrometry. Eur J Pharm Biopharm.

Siakotos, A.N., Rouser, G., 1969. Isolation of highly purified human and bovine brain endothelial cells and nuclei and their phospholipid composition. Lipids 4, 234-239.

Slotte, J.P., 2016. The importance of hydrogen bonding in sphingomyelin's membrane interactions with co-lipids. Biochim Biophys Acta 1858, 304-310.

Stewart, B.H., Chan, O.H., 1998. Use of immobilized artificial membrane chromatography for drug transport applications. J Pharm Sci 87, 1471-1478.

Taillardat-Bertschinger, A., Barbato, F., Quercia, M.T., Carrupt, P.-A., Reist, M., La Rotonda, M.I., Testa, B., 2002. Structural Properties Governing Retention Mechanisms on Immobilized Artificial Membrane (IAM) HPLC Columns. Helvetica Chimica Acta 85, 519-532.

Tsinman, O., Tsinman, K., Sun, N., Avdeef, A., 2011. Physicochemical selectivity of the BBB microenvironment governing passive diffusion--matching with a porcine brain lipid extract artificial membrane permeability model. Pharm Res 28, 337-363.

Valko, K., Bevan, C., Reynolds, D., 1997. Chromatographic Hydrophobicity Index by Fast-Gradient RP-HPLC: A High-Throughput Alternative to log P/log D. Anal Chem 69, 2022-2029.

Vallaro, M., Ermondi, G., Caron, G., 2020. Chromatographic HILIC indexes to characterize the lipophilicity of zwitterions. Eur J Pharm Sci 145, 105232.

Van Bree, J.B., De Boer, A.G., Danhof, M., Breimer, D.D., 1992. Drug transport across the blood--brain barrier. I. Anatomical and physiological aspects. Pharm Weekbl Sci 14, 305-310.

Verzele, D., Lynen, F., De Vrieze, M., Wright, A.G., Hanna-Brown, M., Sandra, P., 2012. Development of the first sphingomyelin biomimetic stationary phase for immobilized artificial membrane (IAM) chromatography. Chem Commun (Camb) 48, 1162-1164.

Wishart, D.S., Feunang, Y.D., Guo, A.C., Lo, E.J., Marcu, A., Grant, J.R., Sajed, T., Johnson, D., Li, C., Sayeeda, Z., Assempour, N., Iynkkaran, I., Liu, Y., Maciejewski, A., Gale, N., Wilson, A., Chin, L., Cummings, R., Le, D., Pon, A., Knox, C., Wilson, M., 2018. DrugBank 5.0: a major update to the DrugBank database for 2018. Nucleic Acids Res 46, D1074-D1082.